

# Hand-gesture-control-based Navigation Using Wearable Armband with Surface Electromyography and Inertial Measurement Unit Sensor Data for Autonomous Guided Vehicles with Robot Operation System-based Simultaneous Localization and Mapping Navigation in Smart Manufacturing

Ing-Jr Ding\* and Ya-Cheng Juang

Department of Electrical Engineering, National Formosa University,  
No.64, Wunhua Rd., Huwei Township, Yunlin County 632, Taiwan, ROC

(Received June 25, 2022; accepted September 13, 2022)

**Keywords:** hand gesture recognition, ANN, SEMG, IMU, ROS-based SLAM, AGV

Autonomous guided vehicles (AGVs) with a robot operation system (ROS)-based platform have been widely used in automation-assisted manufacturing. AGV robots in smart manufacturing are mainly used to handle materials. Such AGV robots with an ROS are generally capable of simultaneous localization and mapping (SLAM) and can therefore perform autonomous navigation (the well-known ROS-based SLAM navigation). From the viewpoint of “smart” manufacturing, which is expected to have richer artificial intelligence and human–robot interaction (HRI), an AGV robot with only ROS-based SLAM autonomous navigation is extremely restricted in functions and human–robot interactions. In this work, to increase HRIs and the flexibility of usage of AGVs with only ROS-based SLAM autonomous navigation, a hand-gesture-control-based navigation approach using a wearable armband with sensor data from both surface electromyography (SEMG) and an inertial measurement unit (IMU) is presented. The developed hand-gesture-control-based navigation with artificial neural network (ANN) hand gesture command recognition can be incorporated into a typical AGV operation with SLAM autonomous navigation. The hand-gesture-control-based navigation for AGVs proposed in this study mainly consists of two calculation phases: the detection of the significant hand gesture for the corresponding gesture operation command by the analysis of eight-axis SEMG data, and the recognition of hand gesture commands from the operator using an ANN with nine-axis IMU data. To appropriately combine the detection and recognition of hand gestures, two strategies were developed for the navigation control of an AGV in a certain continuous time period: ANN recognition by the IMU in a fixed decision window with an SEMG system wake-up, and ANN recognition by the IMU in a variable decision window with both a system wake-up and end. A series of online test experiments on AGV navigation by hand gesture control demonstrated that the presented approach has a competitive performance, particularly for short-path navigation.

---

\*Corresponding author: e-mail: [eugen.ding@gmail.com](mailto:eugen.ding@gmail.com)  
<https://doi.org/10.18494/SAM4045>

## 1. Introduction

Recently, research on sensor devices in micro-electromechanical systems (also known as micro-systems) has turned towards the development of compound sensor devices. Unlike a single-sensor device, a compound sensor device can have numerous types of sensors. A compound sensor device such as a wearable armband sensing device with two different categorizations of sensors for surface electromyography (SEMG) and inertial measurement unit (IMU), the Myo armband made by the Thalmic Labs,<sup>(1)</sup> can be used to construct more advanced artificial intelligence (AI) application systems with smart human–machine interactions (HMIs) such as hand gesture recognition

Meanwhile, the rapid development of micro-system sensor techniques has considerably increased the intelligence of automation equipment. With the auxiliary use of an advanced image sensor, such as light radar (also known as LiDAR), the functionalities and uses of the automation equipment of an autonomous guided vehicle (AGV) can be further extended. Moreover, an AGV with a LiDAR sensor can perform the commonly used function of simultaneous localization and mapping (SLAM).<sup>(2)</sup> AGVs with SLAM navigation are widely used in real-life applications, for example, sweeping robots (cleaning robots) in homes<sup>(3)</sup> and transport vehicles in product line manufacturing.<sup>(4–6)</sup> Nowadays, with the popularity of robot operation system (ROSS) that can support multiple functionalities (including SLAM), AGVs with ROS-based SLAM navigation have attracted considerable interest and are being widely adopted in smart factories.<sup>(7–9)</sup> However, from the viewpoint of autonomous mobile robot (AMR) designs with high flexibility and factory security, AGVs with ROS-based SLAM navigation require further improvement. Such AGVs with ROS-based SLAM navigation may be dangerous in unexpected situations and place serious restrictions on task plans without high manufacturing flexibility. To tackle this issue, in this work, we significantly increased the smartness of human–robot interactions on AGVs with ROS-based SLAM navigation by developing and incorporating hand-gesture-control-based AGV navigation using the Myo armband with SEMG and IMU gesture-sensing characteristics (see Fig. 1). The AGV system adopted in this study is the well-known TurtleBot wheeled-vehicle robot with the version 1 ROS, where an additional design is appropriately used to carry the material.<sup>(10)</sup> The ROS-based SLAM autonomous navigation on such a wheeled-vehicle robot that can be operated concurrently with the presented hand-gesture-command-based navigation is finely regulated by the well-known “gmapping” SLAM approach, which is categorized into the 2D-SLAM type.<sup>(11)</sup>

Studies on the use of wearable armbands or bracelets with specific sensors to acquire gestures for the development of smart applications have been frequently reported, with studies focusing on healthcare,<sup>(12,13)</sup> rehabilitation,<sup>(14)</sup> entertainment, and virtual reality (VR).<sup>(15)</sup> Such wearable sensor devices have rarely been used in studies to establish a hand-gesture-based human–robot interaction scheme for a target robot device for smart manufacturing. In addition, most studies related to AGV techniques have been aimed at enhancing the typical SLAM approach (including mapping, AGV localization, and AGV obstacle avoidance improvements) and to implement tasks related to AGV SLAM navigation integrated in a specific environment.<sup>(16,17)</sup> There have been few reports on the development of a hand-gesture-based

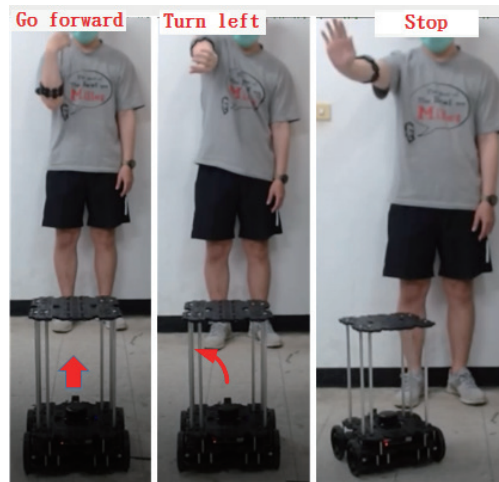


Fig. 1. (Color online) Incorporation of human–robot interactions in AGV platform with ROS-based SLAM navigation by developing a hand-gesture-control-based AGV navigation scheme.

command scheme using a wearable armband sensing device for implementation in AGV SLAM navigation. In our previous study,<sup>(12)</sup> the Myo armband was used to develop a service robot system with specialized hand-gesture-based human–computer interfaces for people with mobility problems. In this study, only the Myo armband software development kit (SDK) was used to provide various recognizable gesture commands to construct the application (a two-layer hierarchy scheme to significantly increase hand gesture command numbers presented for implementing real-life applications) and for operator identity recognition. Although vehicle robot navigation and positioning were also discussed in Ref. 12, the presented approaches did not involve hand gesture control. In contrast to Ref. 12, considering the effective and efficient utilization of AGVs in a smart factory, in this study, we develop a hand-gesture-control-based navigation system using a wearable armband to acquire SEMG and IMU sensing data for an AGV with ROS-based SLAM navigation, as discussed in Sect. 2.

## 2. Hand-gesture-control-based Navigation Using Wearable Armband with SEMG and IMU Sensing Data for AGV with ROS-based SLAM Navigation

In this section, the developed hand-gesture-control-based navigation approach for a typical AGV platform with ROS-based SLAM navigation is described in detail. The proposed hand-gesture-control-based navigation for the AGV essentially belongs to the recognition-based technique category (i.e., a complete gesture command action classified by the system) with the motion of the target vehicle completely regulated in accordance with the recognized gesture command from the operator. In the proposed scheme, the operator wears the Myo armband to continually acquire sensed activity data to perform the desired gesture command for controlling the AGV. To ensure effective control of the AGV without concern about false alarms (i.e., AGV motion driven by an unintended hand gesture), the system was designed to be able to understand

the starting and ending timestamps of the data acquisition of the provided hand gesture command. Both the wake-up and end calls of the hand gesture recognition system are presented in this paper. In addition, to achieve smart and flexible AGV navigation, the proposed hand-gesture-control-based navigation approach was incorporated in an AGV with typical ROS-based SLAM navigation. A master–slave AGV vehicle navigation management strategy is also presented.

## 2.1 Acquisition of SEMG and IMU sensor information from wearable Myo armband

As mentioned in the previous section, the Myo armband was used in this work to acquire hand gesture activity data,<sup>(1)</sup> mainly the data of the SEMG and IMU sensors. Figures 2 and 3 depict the eight-axis SEMG electrodes (a total of eight sensors set in a ring formation around the wearable device) and the nine-axis IMU sensor (including the three-axis accelerator, three-axis gyroscope, and three-axis magnetometer), respectively. As shown in Fig. 2, the operator wears the Myo armband on the upper forearm. When the operator extends their upper forearm, the eight-axis SEMG sensing data ( $SEMG_i$ ,  $i = 1, 2, \dots, 8$ , labeled in Fig. 2) are not zero values again and become active and variable from the immediate variations of the surface, and the muscle strength is obtained from the device. When the operator wearing the armband makes an arbitrary hand gesture, information about the variation of this gesture is acquired from the nine-axis IMU sensor in the device. Such variations in the gesture mainly contain information of the acceleration (from the three-axis accelerator) and the rate of angular change (from the three-axis gyroscope). As shown in Fig. 3, the three-axis accelerator data represent the variation in acceleration in the 3D ( $x, y, z$ ) space when a gesture is performed; the data derived from the three-axis gyroscope contain variations in the angle in three different dimensions, namely roll, pitch, and yaw. The roll–pitch–yaw angle is also known as the Euler angle, which can be used to effectively describe rotation features, including the hand gestures with hand rotations in this work. Note that a typical IMU sensor has six axes because it employs a three-axis accelerator and a three-axis gyroscope. In contrast to typical six-axis IMUs, the Myo armband adopted in this work also has a three-axis magnetometer. To acquire hand gesture information, the sensing data from the three-axis magnetometer are used to help the gyroscope solve the problem that gravitational acceleration does not provide information on horizontal angle rotation. The nine-axis IMU information (denoted  $Myo-IMU_i$ ,  $i = 1, 2, \dots, 9$ ) for describing the varying



Fig. 2. (Color online) SEMG sensor data acquisition with the wearable Myo armband for implementing the system wake-up call of the hand gesture recognition system (eight-axis SEMG).

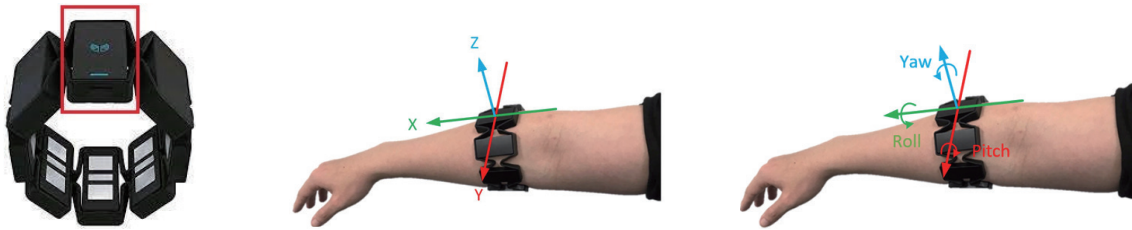


Fig. 3. (Color online) IMU sensor data acquisition with the Myo armband for calculations of hand gesture recognition (nine-axis IMU with three-axis accelerometer, three-axis gyroscope, and three-axis magnetometer).

characteristics of different hand gestures is used to establish artificial neural network (ANN)-based hand gesture command recognition for hand-gesture-control-based AGV navigation, as discussed in detail in the following section.

## 2.2 Hand gesture command recognition by ANN classification models with nine-axis IMU information for hand-gesture-control-based AGV navigation

Figure 4 illustrates the structure of the newly established ANN-based hand gesture command recognition system for hand-gesture-control-based AGV navigation. The constructed ANN recognition system was designed as a 9-8-9-5 calculation framework, in which four layers are included: the nine-node input layer for receiving the nine-axis IMU information from the Myo armband, the first hidden layer with eight nodes, the second hidden layer with nine nodes, and the five-node output layer for indicating five different types of hand gesture commands to navigate the target vehicle. As shown in Fig. 4, the outputs from the output layer of the constructed ANN were  $y_1$ ,  $y_2$ ,  $y_3$ ,  $y_4$ , and  $y_5$ , which indicated five different hand gesture commands to regulate vehicle motions, namely, forward increment, backward increment, clockwise increment, counterclockwise increment, and robot stop, respectively.

Note that in the development of the ANN-based hand gesture command recognition system in this study, a dynamic hand gesture command is represented by a series of nine-axis IMU datasets observed within a certain time period with  $n$  continuous timestamp samples (of 1 s duration with  $n = 50$  set in this work). To be able to send the IMU information of  $n$  continuous samples in one time period to the ANN for gesture command classification,  $\overline{Myo-IMU}_i$  in Eq. (1) is estimated to accumulate  $n$  continuous IMU sets,

$$\overline{Myo-IMU}_i = \sqrt{\frac{\sum_{j=1}^n Myo-IMU_{ij}^2}{n}}, \quad i = 1, 2, \dots, 9, \quad (1)$$

where  $\overline{Myo-IMU}_i$  is the estimated root mean square value for all  $n$  collected IMU samples. Using Eq. (1), a continuous-time hand gesture command with  $n$  continuous nine-axis IMU sets can be represented in the simple form  $\{\overline{Myo-IMU}_1, \overline{Myo-IMU}_2, \dots, \overline{Myo-IMU}_9\}$ , which



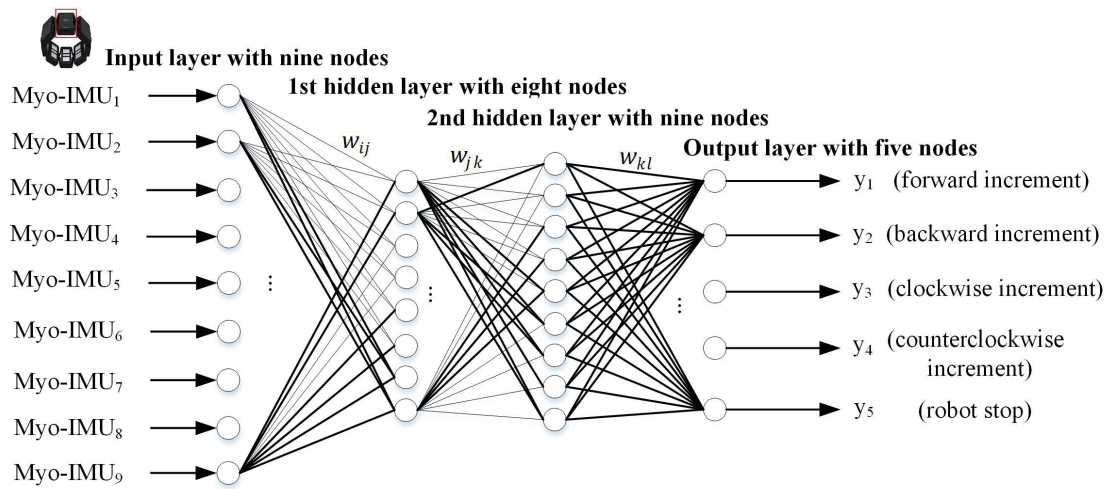


Fig. 4. 9-8-9-5 ANN with nine input nodes (nine-axis IMU data obtained from the Myo armband), first hidden layer of eight nodes, second hidden layer of nine nodes, and output layer of five nodes (five gesture commands).

denotes the 9D feature parameter vector used for training and testing the ANN model used to classify the five hand gesture commands. In the training phase to establish the ANN hand gesture classification models, the backpropagation approach for model optimization was adopted. In addition, a sigmoid-type activation function is used in the output of each neuron of the constructed ANN, and the soft-max scheme is adopted for decisions in the output layer.

In the design part of the AGV navigation, we designed a driverlike control scheme for AGV navigation using recognized hand gesture commands. Under the regulation of the presented vehicle control scheme, the target vehicle can perform the actions of “speed-up forward in a straight line”, “slow-down forward in a straight line”, “speed-up backward in a straight line”, “slow-down backward in a straight line”, “speed-up in a clockwise turn”, “slow-down in a clockwise turn”, “speed-up in a counterclockwise turn”, “slow-down in a counterclockwise turn”, and “stop immediately”. Such fine vehicle control design by hand gestures is similar to real vehicle-driving behavior with the common actions of “step on gas pedal to increase vehicle velocity”, “release gas pedal to decrease vehicle velocity”, “turn steering wheel left to move vehicle left”, “turn steering wheel right to move vehicle right”, and “pull handbrake to stop vehicle”.

To achieve the above-mentioned vehicle regulation, in this work, the motion state of the vehicle is defined to include five different types: completely stopped (State-1, S1), moving forward (State-2, S2), moving backward (State-3, S3), moving right (State-4, S4), and moving left (State-5, S5). Initially, the vehicle is in state S1. In this scenario, the operator gives the gesture command of “forward increment” to change the state to S2, whereas if the gesture command of “backward increment” is made by the operator, the vehicle state changes to S3. In S2, the operator can still give the gesture command of “forward increment” or “backward increment” to speed up and slow down the vehicle, respectively. In S3, the velocity is increased in the backward direction by a series of “backward increment” gesture commands. The gesture

command of “forward increment” can also be used in S3 to decrease the backward vehicle velocity. In both S2 and S3, the gesture commands “clockwise increment” and “counterclockwise increment” can also be given to change the states of the straight-line movement to S4 and S5, respectively. In states S2, S3, and S4, the vehicle can be given the gesture command “robot stop” to make the vehicle enter S1. Equations (2)–(9) show such regulations on movements and rotations of the AGV.

$$\text{Forward speed-up: } forward\_speed(t) = forward\_speed(t-1) + forward\_gain \quad (2)$$

$$\text{Forward slow-down: } forward\_speed(t) = forward\_speed(t-1) - backward\_gain \quad (3)$$

$$\text{Backward speed-up: } backward\_speed(t) = backward\_speed(t-1) + backward\_gain \quad (4)$$

$$\text{Backward slow-down: } backward\_speed(t) = backward\_speed(t-1) - forward\_gain \quad (5)$$

$$\text{Right speed-up: } right\_angle(t) = right\_angle(t-1) + clockwise\_gain \quad (6)$$

$$\text{Right slow-down: } right\_angle(t) = right\_angle(t-1) - counterclockwise\_gain \quad (7)$$

$$\text{Left speed-up: } left\_angle(t) = left\_angle(t-1) + counterclockwise\_gain \quad (8)$$

$$\text{Left slow-down: } left\_angle(t) = left\_angle(t-1) - clockwise\_gain \quad (9)$$

Note that in these equations, the indexes *forward\_gain*, *backward\_gain*, *clockwise\_gain*, and *counterclockwise\_gain* have positive values, all of which are determined by a simple procedure and are used to change the motion state of the vehicle motor. These four indexes are delivered when obtaining recognized gesture commands of forward increment ( $y_1$ ), backward increment ( $y_2$ ), clockwise increment ( $y_3$ ), and counterclockwise increment ( $y_4$ ), respectively.

### 2.3 Hand-gesture-control-based AGV navigation using ANN hand gesture command recognition with SEMG-driven system wake-up and end

In this section, we discuss the use of the above-mentioned hand-gesture-control-based AGV navigation by ANN hand gesture command recognition in a practical online application. Note that when the hand gesture recognition system was used in a real-life application, the main problem was the acquisition of significant hand gesture command samples, i.e., the extraction of a meaningful gesture command segment with continuous-time nine-axis IMU data. To address this issue, two approaches were developed to finely extract the practical hand gesture command segment provided by the operator to classify gesture navigation commands: (1) an SEMG-driven system wake-up with a fixed-size IMU segment for ANN hand gesture command recognition and (2) an SEMG-driven system wake-up and end with a variable-size IMU segment for ANN hand gesture command recognition.

Table 1 shows that in the scenario wherein the operator with the Myo armband exerted strength within a certain short time period (1 s), all sample amplitudes of the eight SEMG channels around the Myo armband—SEMG1, SEMG2, ..., and SEMG8—were obtained (50 samples obtained in each SEMG channel with the sampling rate set at 50). Using all the observed data presented in Table 1, the sample amplitude curve of each of the eight SEMG channels was then further acquired and plotted, as shown in Fig. 5. Figure 5 shows that when a significant hand gesture command was performed, the fluctuations of the amplitude values of each SEMG channel in the axis of the sample timestamp were similar. Accordingly, a calculated SEMG sample representative of all eight SEMG samples was acquired. Representative SEMG samples were obtained using

$$SEMG_{Detect} = \sqrt{\frac{SEMG1^2 + SEMG2^2 + \dots + SEMG8^2}{8}}, \quad (10)$$

where the calculated term  $SEMG_{Detect}$  indicates the estimated value of the root mean square calculations on the sensing data of all eight SEMG channels of the Myo armband. In the SEMG-driven system wake-up with the fixed-size IMU segment for ANN hand gesture command recognition,  $SEMG_{Detect}$  derived from Eq. (10) was used to estimate the starting timestamp of the performed gesture command (i.e., wake up the gesture command recognition system);

Table 1

Eight-axis SEMG information collected in time period of 1 s, in which sample strength (amplitude) variations of eight channels, SEMG1, SEMG2, ..., and SEMG8, are provided (50 consecutive samples collected in eight SEMG channels, IMU sampling rate of Myo armband set as 50).

	SEMG1	SEMG2	SEMG3	SEMG4	SEMG5	SEMG6	SEMG7	SEMG8
Sample-1	-4	2	-1	2	-1	-1	0	-1
Sample-2	-3	-1	-3	0	-2	-2	0	-2
Sample-3	-1	-3	-4	6	-1	0	-2	-1
⋮				⋮				
Sample-48	-22	23	14	-13	-54	-81	-128	-30
Sample-49	55	-55	94	80	24	-82	-59	71
Sample-50	54	-48	-24	-36	-81	-63	102	-63

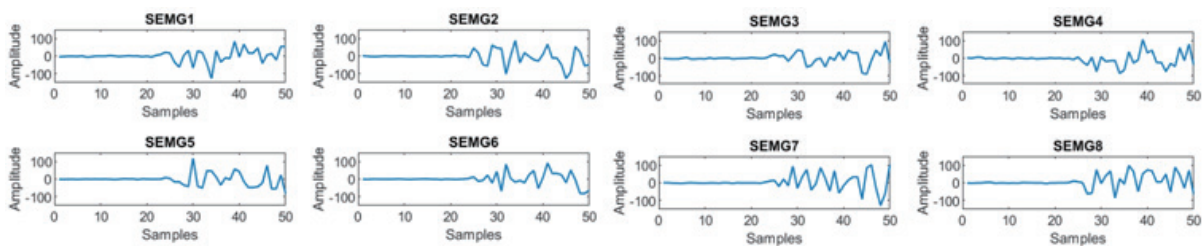


Fig. 5. (Color online) Sample amplitude curves of eight SEMG channels around Myo armband when operator exerts strength in time period of 1 s (IMU sampling rate set as 50).



furthermore, it was used to evaluate both the starting and ending timestamps of the gesture command made by the operator (i.e., wake-up and final ending gesture command recognition) in the SEMG-driven system wake-up and the end with the variable-size IMU segment for ANN hand gesture command recognition.

As shown in Fig. 6(a), the presented hand-gesture-controlled AGV navigation by ANN hand gesture command recognition with the fixed-size IMU segment is incorporated with a typical ROS-based SLAM navigation scheme. When the operator wakes up the gesture recognition system by exerting significant strength in the upper forelimb, the estimated term  $SEMG_{Detect}$  from the Myo armband becomes of interest; if  $SEMG_{Detect}$  is larger than the set threshold value

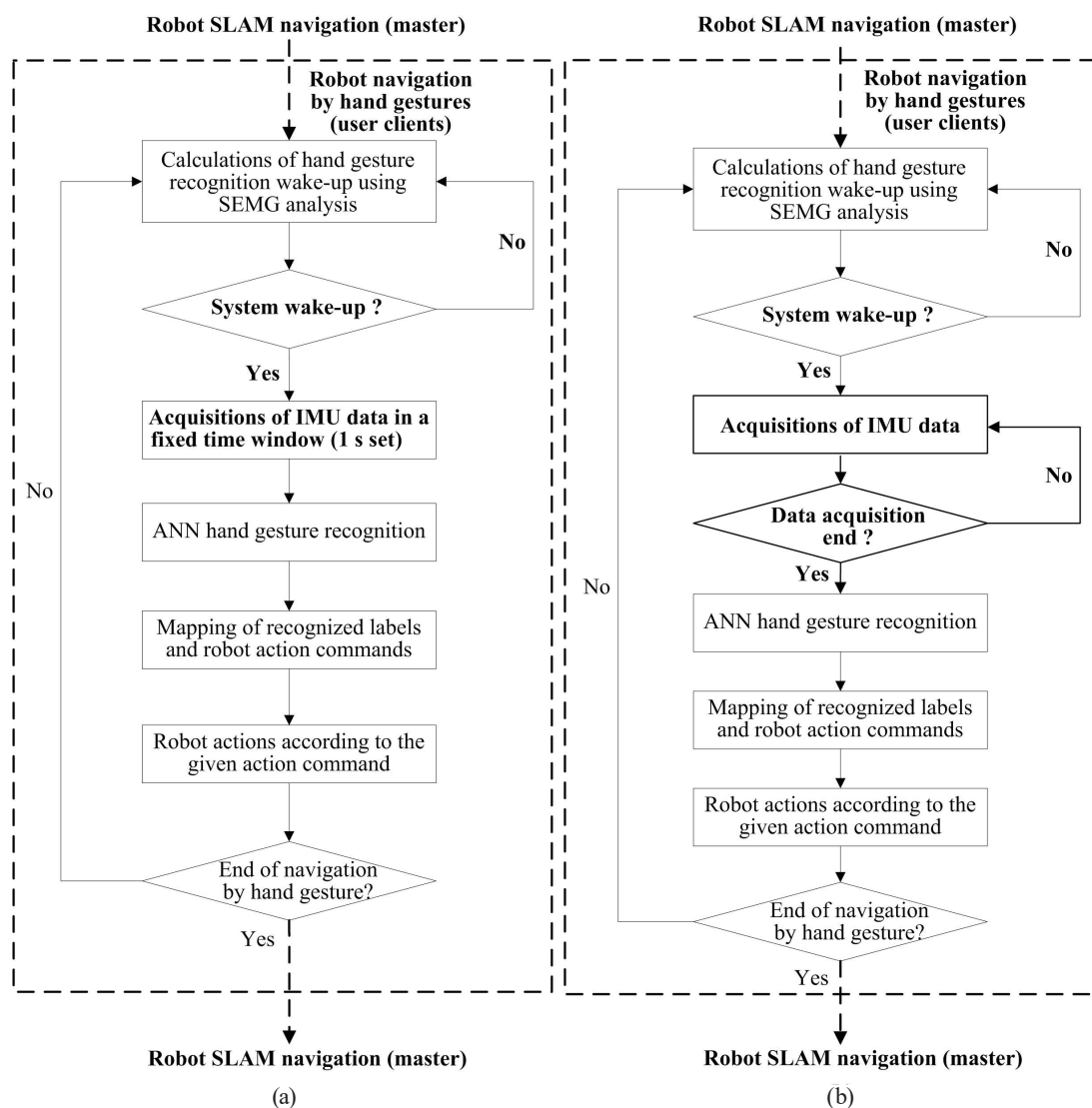


Fig. 6. Strategies developed for AGV navigation control during a continuous time period by ANN recognition using IMU data contained (a) in “fixed” decision window where the SEMG-driven system wake-up is considered alone (approach with extraction of the “fixed-size” IMU segment) and (b) in the “variable” decision window where both system wake-up and end are carried out (approach with extraction of the “variable-size” IMU segment).

(denoting successful system wake-up), the system is triggered to start to acquire consecutive IMU samples of the gesture (following the significant strength exerted, a specific gesture command is made by the operator). Note that in the scheme presented in Fig. 6(a), the extracted segment of consecutive IMU samples has a fixed size (i.e., a fixed time duration designed to collect IMU action samples for recognition; this duration was set to 1 s in this work). Different from this design with fixed-size IMU segment extraction, another design that uses a variable-size window to collect IMU action samples is depicted in Fig. 6(b). As shown in Fig. 6(b), upon the additional importing of the IMU detection,  $IMU_{Detect}$ , expressed in Eq. (11), the time period of the collected IMU action samples, which is the duration of the timestamps of system waking-up expressed by Eq. (10) and the system end expressed in Eq. (11), becomes variable. The estimate of the term  $IMU_{Detect}$  is similar to the term  $SEMG_{Detect}$  used in the system wake-up phase (i.e., the root mean square calculations on the sensing data) and is used for estimating the end of IMU action sample extraction (i.e., the timestamp of the finished gesture command).

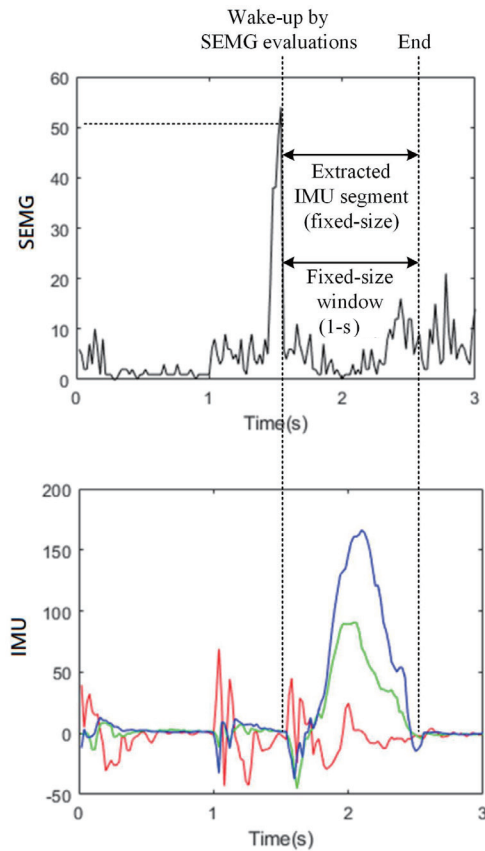
$$IMU_{Detect} = \sqrt{\frac{IMU1^2 + IMU2^2 + \dots + IMU9^2}{9}} \quad (11)$$

Note that in the scheme of SEMG-driven system wake-up and end with the variable-size IMU segment, after system wake-up, IMU samples of the gestures made by the operator are continually acquired until the system end is finally reached by  $IMU_{Detect}$  evaluation. As shown in Fig. 6(b), similar to the  $SEMG_{Detect}$  evaluation in the use of system wake-up,  $IMU_{Detect}$  evaluation is conducted during the period of hand gesture making, and when  $IMU_{Detect}$  is smaller than the set threshold value (denoting the completion of the operated command), IMU sample extraction is ended immediately, and the collected IMU samples are sent to the ANN hand gesture recognition calculations for gesture command classification. Figure 7 illustrates the difference between the presented fixed-size and variable-size window schemes in the collection of meaningful IMU gesture command samples in real-life applications for navigating the AGV.

#### 2.4 Hand-gesture-control-based navigation incorporating ROS-based SLAM autonomous navigation for AGV in smart manufacturing

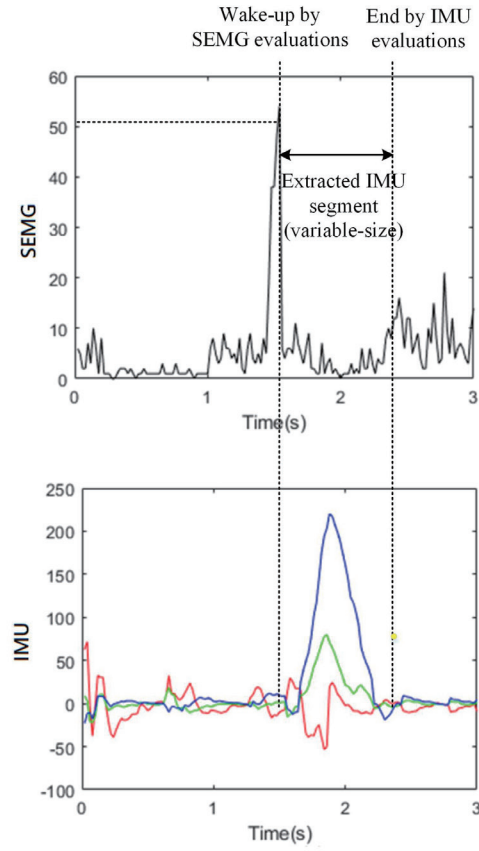
ROS-based SLAM navigation was further incorporated into the design of the presented hand-gesture-control-based AGV navigation by ANN hand gesture command recognition with wake-up and end detection of gesture data acquisition detailed in the previous section. The AGV platform with two types of navigation of the typical SLAM and the proposed hand gesture command control has considerably more flexibility than that with only the SLAM navigation alone in practical applications, enabling more complicated navigation paths and safer services with fewer dangerous incidents in real-life applications. To enable the AGV to achieve such dual navigation, we propose a master–slave AGV navigation management scheme. As shown in Fig. 8, in such a scheme, one master (i.e., ROS robot master) and multiple slaves (i.e., operator slaves) are contained. The mission of the ROS robot master has been to perform typical ROS-based SLAM navigation on the AGV, and each operator slave defined in the scheme can regulate the AGV by hand-gesture-command-controlled AGV navigation. Note that in the presented

Extraction of fixed-sized IMU command samples



(a)

Extraction of variable-sized IMU command samples



(b)

Fig. 7. (Color online) Differences in presented (a) fixed-size and (b) variable-size window schemes in collection of meaningful IMU gesture command samples in real-life applications for AGV hand gesture navigation.

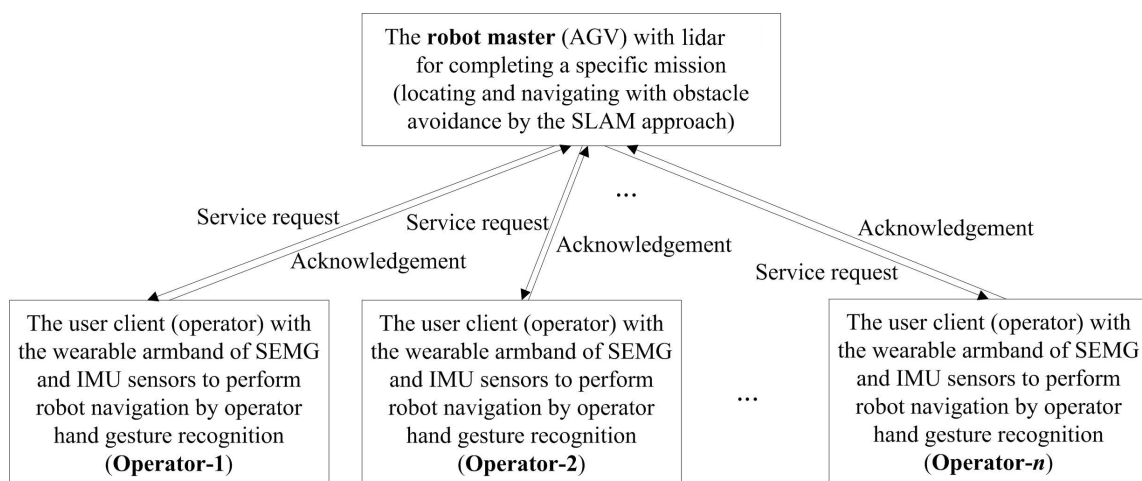


Fig. 8. Master–slave scheme for regulating SLAM autonomous navigation and hand gesture navigation of operator in practical application scenario with  $n$  operators.

scheme, when an operator desires to control the navigation of the AGV by hand gesture commands, a service request to the robot master is made by the user in advance. Only when the robot master acknowledges the user's request (i.e., the user is permitted to control the AGV) can the AGV then be navigated by hand gesture command control by the permitted user. Using the scheme presented in Fig. 8, the AGV navigation is concurrently regulated by navigation by ROS-based SLAM and by operator hand gesture commands (as shown in Fig. 9). During a continuous time period, only one kind of navigation could be performed on the AGV: either ROS-based SLAM or hand gesture command control (by one of multiple operators).

In the presented master–slave scheme for regulating the SLAM autonomous navigation and hand gesture navigation of the operator, some critical technical issues were considered and governed by effective policies, as summarized below.

- Switch from ROS-based SLAM to hand gesture command control

In the scenario that AGV navigation is switched from ROS-based SLAM of the master to hand gesture command control of a specific operating user, a context switch process that can effectively retain the current executing information of the ROS-based SLAM navigation is considered (i.e., swapping the current SLAM navigation); for this phase, a navigation control block was also precisely designed to contain all types of execution data of SLAM navigation on the AGV.

- Switch from hand gesture command control to ROS-based SLAM

Compared with the above-mentioned issue, the navigation switch to convert the hand gesture command control mode to the ROS-based SLAM mode was given more attention. Under such a condition, the context switch process had to be designed to be able to load the previous execution condition of the ROS-based SLAM navigation (i.e., swapping of the previous SLAM navigations). After loading the previous SLAM navigation information from the navigation control block, the AGV could continue the previously aborted SLAM navigation mission (making the AGV return to the position of the previously aborted SLAM navigation and resuming such navigation). In this phase, for fine AGV navigation management, it was necessary to provide an alternative to making the AGV return to the starting position of the previous SLAM navigation path and restart a new SLAM navigation mission.

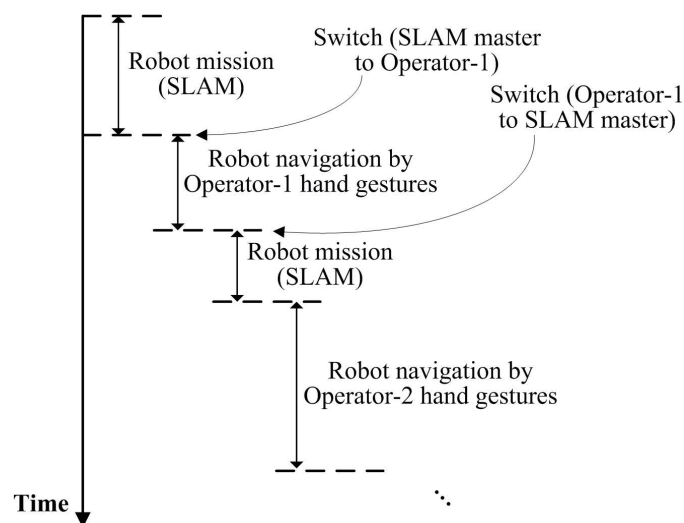


Fig. 9. Enhanced AGV navigation performed with concurrent executions of ROS-based SLAM navigation and hand-gesture-control-based navigation.

- Priority management of multiple AGV navigations

In the proposed scheme, the ROS robot master with SLAM navigation and each of the multiple operator slaves that could perform hand-gesture-control-based navigation were given a suitable priority rank. It is important to have a detailed policy to dispatch all the defined master and slave AGV navigations in accordance with their set priority ranks in the case of an urgent and undisturbed ROS-based SLAM navigation or hand gesture control navigation requested by multiple slave operators simultaneously.

- Interrupt process with the timer design of AGV control

To provide efficient AGV services in an overall consideration when a slave operator can control the AGV by hand gesture control for an excessive duration, it was necessary to impose an appropriate restriction on AGV usage. A feasible way to tackle this issue is to set an appropriate timer in the presented AGV navigation scheme, which will be used to regulate the time of hand gesture navigation by each slave operator.

### 3. Experiments

We conducted an experiment on hand-gesture-control-based navigation for an AGV with ROS-based SLAM navigation using a wearable armband to acquire SEMG and IMU sensor data in an office laboratory. We used the popular TurtleBot wheeled-vehicle robot with the ROS system (also known as TurtleBot3). The robot system of TurtleBot3 has two types of models, the Burger type and the Waffle-Pi type; the latter was adopted in this study. The robot contained 360° LiDAR for SLAM navigation, a single-board computer for simple data computation, an open-source control module (OpenCR) for robot motor control, a plate to hold the other components, and a rechargeable battery.<sup>(10)</sup> As shown in Fig. 10(a), a scenario to simulate a factory or manufacturing field was established in the laboratory, where we deployed an AGV with the ability of ROS-based SLAM navigation, and an operator wearing the Myo armband controlled the AGV navigation via recognized hand gesture commands. Figure 10(b) depicts the scene-depth graph of the laboratory, which was obtained using LiDAR of the AGV by the ROS

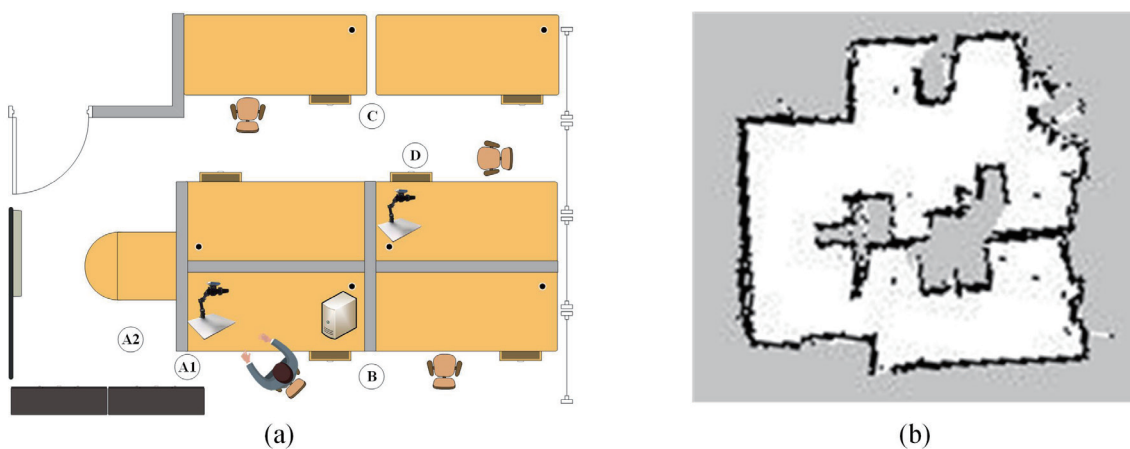


Fig. 10. (Color online) (a) Laboratory scenario for performing AGV-robot SLAM incorporated with wearable SEMG-IMU hand gesture command recognition-based navigation and (b) map constructions made by AGV-robot SLAM (the scene-depth map of the laboratory office environment constructed for automatic navigation of the AGV robot).



SLAM approach. As seen in Fig. 10(b), autonomous navigation of the AGV from the starting location to the destination location was successful using the ROS SLAM approach. In the experiment, the AGV navigation was planned to contain the typical ROS-based SLAM navigation and the hand-gesture-control-based navigation. As shown in Fig. 10(a), the former autonomous navigation paths were set to be from C to B and from B to C (i.e., starting at C and ending at B and starting at B and ending at C, respectively); the later operator-controlled navigation paths were set to be from A2 to A1 and from A2 to D (i.e., starting at A2 and ending at A1 and starting at A2 and ending at D, respectively). Tables 2 and 3 show the results of autonomous ROS-based SLAM navigation of the AGV from C to B and from B to C,

Table 2

(Color online) Scene-depth images derived from automatic navigation of AGV-robot SLAM from C to B in continuous time period.

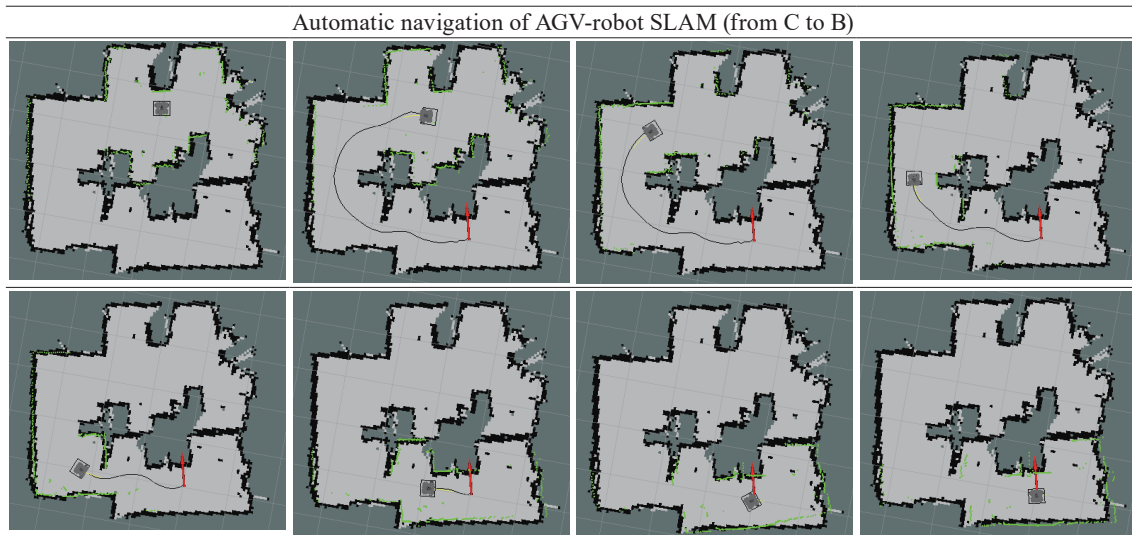
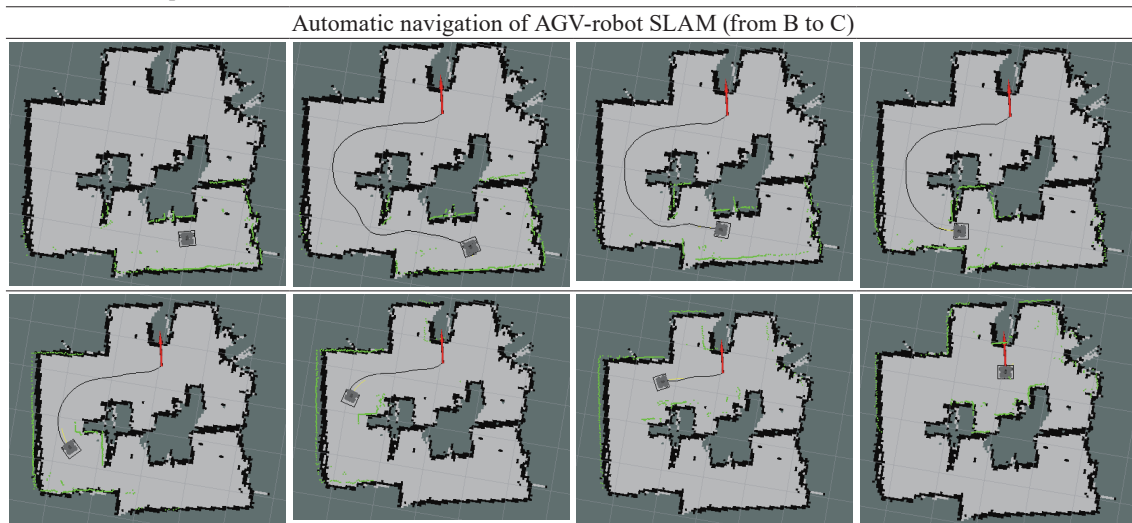


Table 3

(Color online) Scene-depth images derived from automatic navigation of AGV-robot SLAM from B to C in continuous time period.



respectively, during which a series of detailed scene-depth images were derived from the LiDAR of the AGV. The experimental results of AGV navigation by hand gesture control of the operator are described in the following.

Table 4 shows five different categorizations of hand gesture commands used for AGV navigation. As shown in Table 4, these gestures are assigned the labels Label 1 to Label 5, denoting the AGV control commands of “Speed-up forward”, “Speed-up backward”, “Speed-up in a counterclockwise turn”, “Speed-up in a clockwise turn”, and “Stop immediately”, respectively. As mentioned in Sect. 2.2, these gesture commands were classified using the ANN recognition model. Table 5 presents the recognition accuracy of the constructed ANN model for the nine-axis IMU hand gesture classification. Note that in the ANN recognition experiments, the database contained 750 gesture commands, 150 of which were collected for each of the five gesture commands; of the 150 recorded actions for each command, half were used for ANN

Table 4  
(Color online) Five hand gesture commands used for AGV navigation.


Navigation gesture label	Continuous-time hand gestures with Myo armband of SEMG and IMU
Label 1: Speed-up forward (Slow-down backward)	
Label 2: Speed-up backward (Slow-down forward)	
Label 3: Speed-up in the counter-clockwise turn (Slow-down in a clockwise turn)	
Label 4: Speed-up in a clockwise turn (Slow-down in a counter-clockwise turn)	
Label 5: Stop immediately	

Table 5

Confusion matrix showing perfect recognition performance of established ANN model with inputs of nine-axis IMU hand gesture information for classifications of five hand gesture commands.

	Label 1	Label 2	Label 3	Label 4	Label 5
Label 1	75	0	0	0	0
Label 2	0	75	0	0	0
Label 3	0	0	75	0	0
Label 4	0	0	0	75	0
Label 5	0	0	0	0	75

training and the other half were used as test data to evaluate the outside-test recognition rate of the trained ANN. Table 5 shows that the outside-test ANN recognition performance was 100%. This nine-axis IMU ANN hand gesture recognition system with perfect recognition had a positive effect on the hand-gesture-control-based AGV navigation by ANN gesture command recognition with SEMG-driven system wake-up and end.

Finally, the performance of the presented ANN hand gesture command recognition with SEMG-driven system wake-up and end in the experimental phase of hand-gesture-control-based AGV navigation is listed in Tables 6–17. In this study, three test users (test users 1–3) and two strategies (mission-complete-oriented strategy and time-restriction-oriented strategy) were adopted to evaluate the performance of the presented hand-gesture-control-based AGV navigation approach. The performance results of test users 1–3 are presented in Tables 6–9, Tables 10–13, and Tables 14–17, respectively. The mission-complete-oriented strategy was focused on the completed time duration of the hand-gesture-controlled AGV navigation mission (e.g., in the same mission to complete navigation from A2 to A1 using the presented hand-gesture-control-based AGV navigation approach, different time durations were obtained for each of fixed-size and variable-size IMU data extraction); in the time-restriction-oriented strategy, the main focus of the performance evaluations was the set restricted time duration (i.e., the timer with a fixed size) and the degrees of completion of an indicated mission of hand-gesture-controlled AGV navigations (including evaluations of error values of the straight-line distance difference and the direction angle difference of the AGV final location to the indicated destination location). Figure 11 shows such evaluation criteria. Note that for both strategies, two different navigation missions were used to evaluate the performance: a simple mission to navigate from A2 to A1 [see Fig. 10(a)] and a complicated mission to navigate from A2 to D [also see Fig. 10(a)]. In the time-restriction-oriented strategy, time durations of 5 and 30 s were set for navigating from A2 to A1 and from A2 to D, respectively. As observed from the performance results of test user 1 for the mission-complete-oriented strategy (Tables 6 and 7), AGV hand-gesture-controlled navigation by ANN recognition with fixed-size and variable-size IMU windows could effectively complete both the simple and the complex navigation missions. The average performances of ANN recognition with the variable-size window (5.8 s for A2 to A1 and 31.8 s for A2 to D) were slightly better than those with the fixed-size window (7.8 s for A2 to A1 and 37.2 s for A2 to D). As observed from Tables 8 and 9, the performance results for the time-restriction-oriented strategy revealed that AGV hand-gesture-controlled navigation by ANN recognition with both fixed-size and variable-size IMU windows was competitive. In the simple navigation mission from A2 to A1 (see Table 8), the AGV hand-gesture-controlled

Table 6

Performances of user 1 for AGV hand-gesture-controlled navigation by ANN recognition with fixed-size [Fig. 6(a)] and variable-size [Fig. 6(b)] IMU segment extraction in mission-complete-oriented strategy (simple mission of hand-gesture-controlled navigation from A2 to A1).

Method	Test					
	1st test (s)	2nd test (s)	3rd test (s)	4th test (s)	5th test (s)	Average (s)
Fixed-size IMU data extraction	7	8	8	7	9	7.8
Variable-size IMU data extraction	6	6	6	5	6	5.8

Table 7

Performances of user 1 for AGV hand-gesture-controlled navigation by ANN recognition with fixed-size [Fig. 6(a)] and variable-size [Fig. 6(b)] IMU segment extraction in mission-complete-oriented strategy (complex mission of hand-gesture-controlled navigation from A2 to D).

Method	Test					
	1st test (s)	2nd test (s)	3rd test (s)	4th test (s)	5th test (s)	Average (s)
Fixed-size IMU data extraction	36	36	37	38	39	37.2
Variable-size IMU data extraction	32	32	32	30	33	31.8

Table 8

Performances of user 1 for AGV hand-gesture-controlled navigation by ANN recognition with fixed-size [Fig. 6(a)] and variable-size [Fig. 6(b)] IMU segment extraction in time-restriction-oriented strategy (simple mission of hand-gesture-controlled navigation from A2 to A1 with 5 s time duration).

Method	Test					
	1st test	2nd test	3rd test	4th test	5th test	Average
Fixed-size IMU data extraction	(9.8 cm, 0°)	(10.5 cm, 0°)	(7.2 cm, 0°)	(7.4 cm, 0°)	(8.6 cm, 0°)	(8.7 cm, 0°)
Variable-size IMU data extraction	(3.2 cm, 0°)	(2.6 cm, 0°)	(3 cm, 0°)	(4.2 cm, 0°)	(2.5 cm, 0°)	(3.1 cm, 0°)

Table 9

Performances of user 1 for AGV hand-gesture-controlled navigation by ANN recognition with fixed-size (Fig. 6(a)] and variable-size [Fig. 6(b)] IMU segment extraction in time-restriction-oriented strategy (complex mission of hand-gesture-controlled navigation from A2 to D with 30 s time duration).

Method	Test					
	1st test	2nd test	3rd test	4th test	5th test	Average
Fixed-size IMU data extraction	(74.3 cm, -3°)	(99.1 cm, 5°)	(90.7 cm, 5°)	(106.2 cm, -5°)	(121.8 cm, 0°)	(98.4 cm, 3.6°)
Variable-size IMU data extraction	(18.5 cm, 10°)	(75.5 cm, 5°)	(43.3 cm, 0°)	(57.7 cm, 0°)	(42.3 cm, 0°)	(47.5 cm, 3°)

Table 10

Performances of user 2 for AGV hand-gesture-controlled navigation by ANN recognition with fixed-size [Fig. 6(a)] and variable-size [Fig. 6(b)] IMU segment extraction in mission-complete-oriented strategy (simple mission of hand-gesture-controlled navigation from A2 to A1).

Method	Test					
	1st test (s)	2nd test (s)	3rd test (s)	4th test (s)	5th test (s)	Average (s)
Fixed-size IMU data extraction	7	8	7	8	10	8
Variable-size IMU data extraction	6	6	7	6	6	6.2

Table 11

Performances of user 2 for AGV hand-gesture-controlled navigation by ANN recognition with fixed-size [Fig. 6(a)] and variable-size [Fig. 6(b)] IMU segment extraction in mission-complete-oriented strategy (complex mission of hand-gesture-controlled navigation from A2 to D).

Method	Test					
	1st test (s)	2nd test (s)	3rd test (s)	4th test (s)	5th test (s)	Average (s)
Fixed-size IMU data extraction	38	42	42	39	38	39.8
Variable-size IMU data extraction	35	35	35	33	33	34.2

Table 12

Performances of user 2 for AGV hand-gesture-controlled navigation by ANN recognition with fixed-size [Fig. 6(a)] and variable-size [Fig. 6(b)] IMU segment extraction in time-restriction-oriented strategy (simple mission of hand-gesture-controlled navigation from A2 to A1 with 5 s time duration).

Method	Test					
	1st test	2nd test	3rd test	4th test	5th test	Average
Fixed-size IMU data extraction	(10.3 cm, 0°)	(10.5 cm, 0°)	(9.5 cm, 0°)	(7.6 cm, 0°)	(6.1 cm, 0°)	(8.8 cm, 0°)
Variable-size IMU data extraction	(3.2 cm, 0°)	(2.6 cm, 0°)	(3 cm, 0°)	(4.2 cm, 0°)	(2.5 cm, 0°)	(3.1 cm, 0°)

Table 13

Performances of user 2 for AGV hand-gesture-controlled navigation by ANN recognition with fixed-size [Fig. 6(a)] and variable-size [Fig. 6(b)] IMU segment extraction in time-restriction-oriented strategy (complex mission of hand-gesture-controlled navigation from A2 to D with 30 s time duration).

Method	Test					
	1st test	2nd test	3rd test	4th test	5th test	Average
Fixed-size IMU data extraction	(151.2 cm, -5°)	(131.7 cm, 10°)	(140.5 cm, -5°)	(139.9 cm, 10°)	(132.2 cm, 5°)	(139.1 cm, 7°)
Variable-size IMU data extraction	(72.5 cm, 10°)	(136.7 cm, 5°)	(45.5 cm, 40°)	(19.5 cm, 70°)	(20.3 cm, 80°)	(58.9 cm, 41°)

Table 14

Performances of user 3 for AGV hand-gesture-controlled navigation by ANN recognition with fixed-size [Fig. 6(a)] and variable-size [Fig. 6(b)] IMU segment extraction in mission-complete-oriented strategy (simple mission of hand-gesture-controlled navigation from A2 to A1).

Method	Test					
	1st test (s)	2nd test (s)	3rd test (s)	4th test (s)	5th test (s)	Average (s)
Fixed-size IMU data extraction	8	8	9	8	8	8.2
Variable-size IMU data extraction	7	6	6	6	6	6.2

Table 15

Performances of user 3 for AGV hand-gesture-controlled navigation by ANN recognition with fixed-size [Fig. 6(a)] and variable-size [Fig. 6(b)] IMU segment extraction in mission-complete-oriented strategy (complex mission of hand-gesture-controlled navigation from A2 to D).

Method	Test					
	1st test (s)	2nd test (s)	3rd test (s)	4th test (s)	5th test (s)	Average (s)
Fixed-size IMU data extraction	46	41	40	38	39	40.8
Variable-size IMU data extraction	36	36	38	35	37	36.4





## 4. Conclusions

In this work, we presented a hand-gesture-control-based AGV navigation approach using the wearable Myo armband with SEMG and IMU sensors. In the proposed approach, an AGV navigation mission was completed using a series of hand gesture commands (mainly move forward, move backward, turn left, turn right, and stop). A recognition system to classify the hand gesture commands was constructed using an ANN with a nine-axis IMU, in which an SEMG-driven system wake-up and end were designed and finely incorporated. The proposed navigation approach has competitive performance and can be incorporated with typical ROS-based SLAM autonomous navigation to enhance the functionality of the AGV and promote smart manufacturing based on human–robot interactions. In contrast with command-based vehicle navigation, a human–robot collaboration approach to achieve more advanced navigation and interactions for AMR devices will be considered in future work.

## Acknowledgments

We acknowledge the support provided by the Ministry of Science and Technology (MOST), Taiwan under Grant MOST 111-2221-E-150-034.

## References

- 1 M. Geryes, J. Charara, A. Skaiky, A. Mcheick, and J.-M. Girault: Proc. 2017 IEEE Int. Conf. Microelectronics (IEEE, 2017) 1–4. <https://doi.org/10.1109/ICM.2017.8268823>
- 2 A. R. Khairuddin, M. S. Talib, and H. Haron: Proc. 2015 IEEE Int. Conf. Control System, Computing and Engineering (IEEE, 2015) 85–90. <https://doi.org/10.1109/ICCSCE.2015.7482163>
- 3 L. Sui and L. Lin: Proc. 2020 IEEE Int. Symp. Autonomous Systems (IEEE, 2020) 223–227. <https://doi.org/10.1109/ISAS49493.2020.9378863>
- 4 J.-F. Weng and K.-L. Su: J. Intell. Fuzzy Syst. **36** (2018) 1. <https://doi.org/10.3233/JIFS-169897>
- 5 Y. Chen, Y. Wu, and H. Xing: Proc. 2017 IEEE Chinese Automation Congress (IEEE, 2017) 6418–6423. <https://doi.org/10.1109/CAC.2017.8243934>
- 6 A. Ziebinski, D. Mrozek, R. Cupek, D. Grzechca, M. Fojcik, M. Drewniak, E. Kyrkjebø, Jerry C.-W. Lin, K. Øvsthus, and P. Biernacki: Proc. Int. Conf. Computational Science (Springer, 2021) 595–608. [https://doi.org/10.1007/978-3-030-77970-2\\_45](https://doi.org/10.1007/978-3-030-77970-2_45)
- 7 A. F. Olalekan, J. A. Sagor, M. H. Hasan, and A. S. Oluwatobi: Proc. 2021 IEEE Int. Conf. Emerging Technology (IEEE, 2021) 1–5. <https://doi.org/10.1109/INCET51464.2021.9456164>
- 8 S. Thale, M. Prabhu, and P. Thakur: Proc. Int. Conf. Automation, Computing and Communication (ITM Web of Conferences, 2020) 01011. <http://doi.org/10.1051/itmconf/20203201011>
- 9 P. Sankalprajan, T. Sharma, H. D. Perur, and P. Sekhar Pagala: Proc. 2020 Int. Conf. Emerging Technology (IEEE, 2020) 1–6. <https://doi.org/10.1109/INCET49848.2020.9154101>
- 10 R. Amsters and P. Slaets: Proc. 10th RiE, Advances in Intelligent Systems and Computing (Springer, 2019) 170–181. [https://link.springer.com/chapter/10.1007/978-3-030-26945-6\\_16](https://link.springer.com/chapter/10.1007/978-3-030-26945-6_16)
- 11 Y. Abdelrasoul, A. B. S. H. Saman, and P. Sebastian: Proc. 2016 2nd IEEE Int. Symp. Robotics and Manufacturing Automation (IEEE, 2016) 1–6. <https://ieeexplore.ieee.org/document/7847825>
- 12 I. J. Ding, R. Z. Lin, and Z. Y. Lin: Comput. Electr. Eng. **69** (2018) 815. <https://doi.org/10.1016/j.compeleceng.2018.02.041>
- 13 I. J. Ding, C. Y. Tsai, and C. Y. Yen: Microsyst. Technol. **28** (2022) 153. <https://doi.org/10.1007/s00542-019-04503-2>
- 14 S. S. Esfahlani and G. Wilson: Proc. 2017 Computing Conf. (IEEE, 2017) 1021–1028. <https://doi.org/10.1109/SAI.2017.8252217>
- 15 J. Chen, C. Liu, R. Cui, and C. Yang: Proc. Int. Conf. Unmanned Systems and Artificial Intelligence (IEEE, 2019). <https://doi.org/10.1109/ICUSAI47366.2019.9124812>
- 16 P. Beinschob and C. Reinke: Proc. Int. Conf. Intelligent Computer Communication and Processing (IEEE, 2015) 245–248. <https://doi.org/10.1109/ICCP.2015.7312637>
- 17 F. Zhou, L. Zhang, C. Deng, and X. Fan: Sensors **21** (2021) 4604. <https://doi.org/10.3390/s21134604>